1 **Measurement report: Oxidation potential of water-soluble**

2 **aerosol components in the southern and northern of Beijing**

4 Wei Yuan[1], Ru-Jin Huang[1], Chao Luo[2], Lu Yang[1], Wenjuan Cao[1], Jie Guo[1], Huinan

5 Yang[2]

7 [1]State Key Laboratory of Loess and Quaternary Geology, Center for Excellence in

8 Quaternary Science and Global Change, Institute of Earth Environment, Chinese

9 Academy of Sciences, Xi'an 710061, China.

10 [2]School of Energy and Power Engineering, University of Shanghai for Science and

11 Technology, Shanghai 200093, China

12 Correspondence: Ru-Jin Huang (rujin.huang@ieecas.cn) and Huinan Yang

13 (yanghuinan@usst.edu.cn)

15 **Abstract**

16   Water-soluble components have significant contribution to the oxidative

17 potential (OP) of atmospheric fine particles, while our understanding of their

18 relationship is still limited. In this study, the water-soluble OP levels in wintertime

19 $PM_{2.5}$ in the south and north of Beijing, representing the difference in sources, were

20 measured with dithiothreitol (DTT) assay. The volume normalized DTT (DTT_v) in the

21 north (3.5 ± 1.2 nmol min^{-1} m^{-3}) was comparable to that in the south (3.9 ± 0.9 nmol

22 min^{-1} m^{-3}), while the mass normalized DTT (DTT_m) in the north (65.3 ± 27.6 pmol

23 min^{-1} μg^{-3}) was almost twice that in the south (36.1 ± 14.5 pmol min^{-1} μg^{-3}). In both

24 the south and north of Beijing, DTT_v was better correlated with soluble elements

25 instead of total elements. In the north, soluble elements (mainly Mn, Co, Ni, Zn, As,

26 Cd and Pb) and water-soluble organic compounds, especially light-absorbing

27 compounds (also known as brown carbon), had positive correlations with DTT_v.

28 However, in the south, the DTT_v was mainly related to soluble As, Fe and Pb. The

29   sources of DTT$_v$ were further resolved using the positive matrix factorization (PMF)

30   model. Traffic-related emissions (39.1%) and biomass burning (25.2%) were the main

31   sources of DTT$_v$ in the south, and traffic-related emissions (> 50%) contributed the

32   most of DTT$_v$ in the north. Our results indicate that vehicle emission was the

33   important contributor to OP in Beijing ambient PM$_{2.5}$ and suggest that more study is

34   needed to understand the intrinsic relationship between OP and light absorbing

35   organic compounds.

36

37   **1 Introduction**

38   Atmospheric fine particulate matter (PM$_{2.5}$) pollution is one of the major global

39   environmental issues, affecting air quality, climate and human health (Huang et al.,

40   2014; Burnett et al., 2018; An et al., 2019; Zheng et al., 2020). The exposure to PM$_{2.5}$

41   was estimated to be responsible for 8.9 million deaths worldwide in 2015, of which

42   28% occurred in China (Burnett et al., 2018). Numerous studies have shown that

43   oxidative stress is one of the main mechanisms underlying the adverse effects of

44   PM$_{2.5}$ on human health (Chowdhury et al., 2019; Lelieveld et al., 2021; Yu et al.,

45   2022b). When entering the human body, PM$_{2.5}$ can induce the production of excessive

46   reactive oxygen species (ROS) (e.g., H$_2$O$_2$, ·OH and ·O$_2^-$), leading to cellular redox

47   imbalance and generating oxidative stress effects. The ability of PM$_{2.5}$ to cause

48   oxidative stress is defined as oxidative potential (OP).

49   The methods to determine the OP of PM$_{2.5}$ include cellular and acellular assays,

50   and acellular methods are more widely used than cellular methods (Charrier and

51   Anastasio, 2012; Xiong et al., 2017; Calas et al., 2018; Bates et al., 2019; Wang et al.,

52   2020b; Campbell et al., 2021; Oh et al., 2023). Among acellular methods, the

53   dithiothreitol (DTT) assay is extensively applied to determine the OP of ambient

54   particles (Charrier and Anastasio, 2012; Xiong et al., 2017; Liu et al., 2018; Wang et

55   al., 2020b; Puthussery et al., 2022; Wu et al., 2022a). DTT is a surrogate of cellular

56   reductants, and the consumption rate of DTT was used to assess the OP of PM$_{2.5}$.

57   Previous studies have shown that organic matters (e.g., water-soluble organic species

58 and PAHs) and some transition metals (e.g., Mn and Cu) are the important

59 contributors to DTT consumption of $PM_{2.5}$ (Charrier and Anastasio, 2012; Verma et

60 al., 2015; Bates et al., 2019; Wu et al., 2022a; Wu et al., 2022b). For example,

61 Charrier and Anastasio (2012) measured the OP of $PM_{2.5}$ in San Joaquin Valley,

62 California and reported that about 80% of DTT consumption was contributed by

63 transition metals. Verma et al. (2015) measured the OP of water-soluble $PM_{2.5}$ in the

64 southeastern United States and reported that about 60% of DTT activity was

65 contributed by water-soluble organic. The mixtures of metals and organics may

66 produce synergistic or antagonistic effects, such as $\cdot O_2^-$ produced from oxidation of

67 DTT by quinones is more efficiently transformed to $\cdot OH$ in the presence of Fe, while

68 the DTT consumption and $\cdot OH$ generation of quinones are reduced in the presence of

69 Cu (Xiong et al., 2017; Yu et al., 2018; Bates et al., 2019).

70 A number of studies have investigated the OP of water-soluble components in

71 $PM_{2.5}$, which show that the average water-soluble OP values in urban areas ranged

72 from 0.1 to 10 nmol min^{-1} m^{-3} (Fang et al., 2016; Liu et al., 2018; Chen et al., 2019;

73 Wu et al., 2022a; Yu et al., 2022a; Xing et al., 2023). Due to the complexity in

74 chemical composition and sources of $PM_{2.5}$ that determine the OP levels, the sources

75 of OP are also diverse (Verma et al., 2015; Bates et al., 2019; Tuet et al., 2019; Yu et

76 al., 2019; Cao et al., 2021). Several studies have investigated the emission sources and

77 ambient samples to identify the sources of OP (Tuet et al., 2019; Yu et al., 2019; Wang

78 et al., 2020b; Cao et al., 2021), which include both primary and secondary sources.

79 For example, Cao et al. (2021) measured the water-soluble OP of $PM_{2.5}$ samples from

80 six biomass and five coal burning emissions in China, with average values of 4.5-7.4

81 and 0.5-2.1 pmol min^{-1} μg^{-1}, respectively. Tong et al. (2018) investigated the OP of

82 secondary organic aerosols (SOA) from oxidation of naphthalene, isoprene and β-

83 pinene with $\cdot OH$ or O_3, which were 104.4 ± 7.6, 48.3 ± 7.9 and 36.4 ± 3.1 pmol min^{-1}

84 μg^{-1}, respectively. Verma et al. (2014) identified the source of water-soluble OP of

85 $PM_{2.5}$ in Atlanta, United States from June 2012 to September 2013 with positive

86 matrix factorization (PMF) and chemical mass balance (CMB) methods, of which

87 biomass burning was the largest contributor. Wang et al. (2020b) quantified the

88 sources of water-soluble OP of $PM_{2.5}$ in Xi'an, China in 2017 using PMF and multiple

89 linear regression (MLR) methods, with significant contributions from secondary

90 sulfates, vehicle emissions and coal combustion. Despite these efforts, comparative

91 studies on the differences in pollution levels and sources of $PM_{2.5}$ OP in different

92 districts are still limited.

93   In this study, the DTT activity of water-soluble matter in $PM_{2.5}$ samples collected

94 simultaneously in the southern and northern of Beijing in January 2018 were

95 measured. The concentration and light absorption of water-soluble organic carbon

96 (WSOC), as well as the concentrations of 14 trace elements and 7 light-absorbing

97 nitroaromatic compounds (NACs) were quantified. The sources of DTT activity were

98 then identified with PMF model. The results acquired in this study provide a

99 comprehensive comparison of $PM_{2.5}$ OP in different districts of Beijing and its

100 connection with organic compounds, trace elements and sources, which could be

101 helpful for further study of the regional differences in the effects of $PM_{2.5}$ on human

102 health.

103

104 **2 Materials and methods**

105 **2.1 Sampling**

106   Ambient 24 h integrated $PM_{2.5}$ filter samples were collected from January 1 to 31,

107 2018 simultaneously in the south (the Dingfuzhuang village (DFZ), Daxing district;

108 39.61°N, 116.28°E) and north (the National Center for Nanoscience and Technology

109 (NCNT), Haidian district; 39.99°N, 116.32°E) of Beijing (Figure S1). The south site

110 is surrounded by agricultural, industrial, and transportation areas, and the north site is

111 surrounded by residential, transportation and commercial areas. $PM_{2.5}$ samples were

112 collected on pre-baked (780 ℃, 3 h) quartz-fiber filters (20.3 × 25.4 cm; Whatman,

113 QM-A, Clifton, NJ, USA) using high-volume $PM_{2.5}$ samplers (1.13 m^{-3} min^{-1}; Tisch,

114 Cleveland, OH, USA) which were placed on the roof of buildings at heights of about

115 5 m (south) and 20 m (north) above the ground. After collection, the samples were

116   wrapped in baked aluminum foils and stored in a freezer (−20 °C) until further

117   analysis.

2.2 Chemical analysis

119   The mass of $PM_{2.5}$ on the filter was measured by a digital microbalance with a

120   precision of 0.1 mg (LA130S-F, Sartorius, Germany) after 24-h equilibration at a

121   constant temperature (20-23 °C) and humidity (35-45%) chamber. Each filter was

122   weighted at least two times, and the deviations for blank and sampled filters among

123   the repetitions were less than 5 and 10 μg, respectively. The $PM_{2.5}$ mass concentration

124   was calculated by dividing the weight difference before and after sampling by the

125   volume of sampled air.

126   For WSOC analysis, one punch (1.5 cm^2 for concentration analysis and 0.526

127   cm^2 for light absorption measurement) of filter was taken from each sample and

128   extracted ultrasonically with ultrapure water (> 18.2 MΩ cm) for 30 min. After, the

129   extracts were filtered with a 0.45 μm PVDF pore syring filter to remove insoluble

130   substances. Finally, the concentration of WSOC was measured with a total organic

131   carbon-total nitrogen analyzer (TOC-L, Shimadzu, Japan; (Ho et al., 2015)) and the

132   light absorption of WSOC was measured by an UV-Vis spectrophotometer equipped

133   with a liquid waveguide capillary cell (LWCC-3100, World Precision Instruments,

134   Sarasota, FL, USA; (Yuan et al., 2020)). The absorption coefficient (Abs) of WSOC

135   were calculated according to formula S1 in the Supporting Information (SI).

136   The total concentration and soluble fraction concentration of 14 trace elements

137   (i.e., Ti, V, Cr, Mn, Fe, Co, Ni, Cu, Zn, As, Sr, Cd, Ba, and Pb) were quantified by an

138   inductively coupled plasma mass spectrometer (ICP-MS, 7700x, Agilent Technologies,

139   USA), and the details are shown in the SI. For soluble fraction concentration analysis,

140   a punch of filter (47 mm diameter) was extracted with ultrapure water and then

141   centrifuged from residues. For total concentration analysis, another filter with same

142   size was used and digestion after added of 10 mL HNO_3 and 1 mL HF. The extracts

143   were then heated and concentrated to ~ 0.1 mL, and diluted to 5 mL with 2% HNO_3.

144   Afterwards, the diluents were filtered with a 0.22 μm PTFE pore syring filter and

145   stored in a freezer (−4 °C) until further ICP-MS analysis.

146   The concentrations of organic markers (including levoglucosan, mannosan,

147   galactosan, hopanes, picene, phthalic acid, isophthalic acid and terephthalic acid) and

148   light-absorbing NACs (including 4-nitrophenol (4NP), 2-methyl-4-nitrophenol

149   (2M4NP), 3-methyl-4-nitrophenol (3M4NP), 4-nitrocatechol (4NC), 3-methyl-5-

150   nitrocatechol (3M5NC), 4-methyl-5-nitrocatechol (4M5NC) and 4-nitro-1-naphthol

151   (4N1N)) were determined by a gas chromatograph–mass spectrometer (GC-MS;

152   Agilent Technologies, Santa Clara, CA, USA) following the method described

153   elsewhere (Wang et al., 2020a), and more details about the analysis can be found in SI.

154   **2.3 Oxidative potential**

155   The DTT assay was applied to determine the oxidative potential of water-soluble

156   components in $PM_{2.5}$ according to the method by Gao et al. (2017). In brief, a quarter

157   of a 47 mm filter was ultrasonically extracted with 5 mL ultrapure water for 30 min

158   and then filtered with a 0.45 μm PVDF pore syring filter to remove insoluble

159   substances. Afterwards, 0.5 mL of the extract was mixed with 1 mL of potassium

160   phosphate buffer (pH = 7.4) and 0.5 mL of 2 mM DTT in a brown vial, and then

161   placed in a water bath at 37 °C. Then, 20 μL of this mixture was taken at designated

162   time intervals (2, 7, 13, 20, and 28 min) and mixed with 1 mL trichloroacetic acid

163   (TCA; 1% w/v) in another brown vial to terminate the reaction. Then, 0.5 mL of 5,5'-

164   dithiobis-(2-nitrobenzoic acid) (DTNB; 2.5 μM) and 2 mL of tris buffer (pH = 8.9)

165   were added to form 2-nitro-5-thiobenzonic acid (TNB) which has light absorption at

166   412 nm. Finally, the absorption of TNB was measured by a LWCC-UV-Vis. The DTT

167   consumption rate was quantified by the remaining DTT concentration at different

168   reaction times. The DTT activities were normalized by the volume of sampled air

169   (DTT_v, nmol min^{-1} m^{-3}) and the mass concentration of $PM_{2.5}$ (DTT_m, pmol min^{-1} $μg^{-1}$).

170   **2.4 Source apportionment**

171   The sources of DTT activities were identified and quantified using PMF model

172   implemented by the multilinear engine (ME-2; (Paatero, 1997)) following the method

173   described in our previous studies (Huang et al., 2014; Yuan et al., 2020). The input

174   data include species concentration (including DTT_v, 14 trace elements and 8 organic

175   markers) and uncertainties.

176

177   **3 Results and discussion**

178   **3.1 DTT activity and concentrations of water-soluble $PM_{2.5}$ components**

179   Figure 1 shows the daily variation of DTT activity, light absorption of WSOC at

180   wavelength 365 nm (Abs_{365}), together with the concentrations of $PM_{2.5}$, WSOC,

181   NACs and total elements in the south and north of Beijing. Their average values are

182   shown in Table S1. Generally, the average values of $PM_{2.5}$, WSOC, Abs_{365}, NACs and

183   total elements were higher in the south than in the north. Specifically, the

184   concentrations of $PM_{2.5}$ and WSOC in the south (122.3 ± 48.9 and 8.1 ± 5.0 μg m^{-3},

185   respectively) were both about two times higher than that in the north (62.3 ± 27.9 and

186   4.0 ± 2.0 μg m^{-3}, respectively), indicating that the proportion of WSOC in $PM_{2.5}$ was

187   similar in the south and north. However, the Abs_{365} in the south was about three times

188   that in the north, indicating that the chemical composition of WSOC was different

189   between the south and north. Previous studies have reported that NACs are the main

190   water-soluble light-absorbing organic compounds (also known as brown carbon, BrC)

191   of $PM_{2.5}$ (Lin et al., 2017; Huang et al., 2020; Li et al., 2020). For the 7 NACs

192   quantified in this study, the total concentration of nitrophenols (4NP, 2M4NP and

193   3M4NP), nitrocatechols (4NC, 3M5NC and 4M5NC), and 4N1N in the south (108.5 ±

194   72.9 ng m^{-3}, 118.5 ± 91.5 ng m^{-3} and 12.4 ± 8.2 ng m^{-3}, respectively) was about three,

195   five and four times, respectively, those in the north (35.5 ± 21.7 ng m^{-3}, 24.1 ± 30.4 ng

196   m^{-3} and 3.1 ± 3.0 ng m^{-3}, respectively). These results indicate that the sources and

197   emission strength of water-soluble organic compounds were different in the south and

198   north of Beijing, suggesting the different contribution of water-soluble organic

199   compounds to DTT activity. The concentration trend of elements was also different

200   between the south and north of Beijing, with Fe > Zn > Ti > Mn > Cu > Ba > Pb >

201   Sr > Cr > As > V > Ni > Cd > Co in the south, and Fe > Ti > Zn > Ba > Mn > Pb >

202   Cu > Cr > Sr > As > Ni > V > Cd > Co in the north. It should be noted that although

203   the content of $PM_{2.5}$, WSOC and total elements measured in this study were higher in

204   the south than in the north, the average DTT_v value in the south (3.9 ± 0.9 nmol min^{-1}

205   m^{-3}) was comparable to that in the north (3.5 ± 1.2 nmol min^{-1} m^{-3}), meanwhile, the

206   average DTT_m value was much higher (1.8 times) in the north (65.3 ± 27.6 pmol min^{-1}

207   μg^{-1}) than in the south (36.1 ± 14.5 pmol min^{-1} μg^{-1}). The lower DTT_m in the south

208   than in the north may be due to that the increased $PM_{2.5}$ in the south contains more

209   substances with no or little contribution to DTT activity, and indicates that the

210   intrinsic OP of $PM_{2.5}$ was higher in the north than in the south. The similar DTT_v

211   values in the south and north indicate that the exposure-relevant toxicity of $PM_{2.5}$ was

212   comparable in the two sites, and the water-soluble DTT_v was not consistent with the

213   content of water-soluble substances.

214   Figure 2 shows the comparison of DTT_v and DTT_m values measured in this study

215   with those measured in other regions of Asia during similar periods. It can be seen

216   that the DTT_v values measured in Beijing (Campbell et al., 2021; Oh et al., 2023; this

217   study) were lower than that in Jinzhou, Tianjin, Yantai, and Shanghai in China, Lahore

218   and Peshawar in Pakistan, and Delhi in India (Liu et al., 2018; Ahmad et al., 2021;

219   Puthussery et al., 2022; Wu et al., 2022a), higher than that in Xi'an, Nanjing,

220   Hangzhou, Guangzhou, and Shenzhen in China, and Gwangju in Korea (Wang et al.,

221   2019; Wang et al., 2020b; Ma et al., 2021; Yu et al., 2022c; Oh et al., 2023; Xing et al.,

222   2023), and comparable with that in Ningbo, China (Chen et al., 2022). Different from

223   DTT_v, the DTT_m value measured in NCNT in Beijing was similar with that in Jinzhou,

224   Tianjin, Yantai, Shanghai and Ningbo in China (Liu et al., 2018; Chen et al., 2022;

225   Wu et al., 2022a), and higher than that in other regions. The differences in DTT_v and

226   DTT_m values in different regions reflect the regional differences in $PM_{2.5}$ exposure

227   risk and intrinsic toxicity, which can be explained by the differences in chemical

228   composition, sources and atmospheric formation processes (Tong et al., 2017; Wong

229   et al., 2019; Daellenbach et al., 2020; Wang et al., 2020b; Cao et al., 2021). For

230   example, Cao et al. (2021) reported the water-soluble DTT activity of $PM_{2.5}$ from

231   biomass and coal burning emissions in China, and the average value of biomass

232   burning (4.5-7.4 pmol min^{-1} μg^{-1}) was much higher than that of coal burning (0.5-2.1

233   pmol min^{-1} μg^{-1}). Tuet et al. (2017) measured the water-soluble DTT activity of SOA

234   generated under different precursors and reaction conditions, with SOA from

235   naphthalene photooxidation under RO_2 + NO-dominant dry reaction conditions had

236   the highest DTT activity.

237   **3.2 Correlation between DTT activity and water-soluble PM$_{2.5}$ components**

238   Figure 3 shows the correlations of DTT$_v$ with PM$_{2.5}$, WSOC and Abs$_{365}$ in the

239   south and north of Beijing. It can be seen that the correlation coefficient between

240   DTT$_v$ and PM$_{2.5}$ was moderate in both the south (r = 0.42) and north (r = 0.45),

241   indicating that the toxicity of particles can not be evaluated solely by the total PM$_{2.5}$

242   concentration. The correlations between DTT$_v$ with WSOC and Abs$_{365}$ were strong in

243   the north (r of 0.69 and 0.70, respectively), while relatively weak in the south (r of

244   0.41 and 0.40, respectively). The high correlations between DTT$_v$ with WSOC and

245   Abs$_{365}$ in the north of Beijing are coincide with previous studies in Xi'an, China and

246   Atlanta, United States (Verma et al., 2012; Chen et al., 2019), and suggest that water-

247   soluble organic matter, especially BrC, has a significant contribution to DTT

248   consumption in the north. Light-absorbing BrC typically has conjugated electrons,

249   making it more likely to transport electrons for catalytic reactions, thereby

250   contributing to DTT activity (Chen et al., 2019; Wu et al., 2022). Further, in the north,

251   the DTT$_v$ was closely related to the concentrations of NACs (r of 0.57 to 0.79) (Figure

252   S2), suggesting that NACs could be important contributors to DTT consumption.

253   Feng et al. (2022) reported the positive correlations between NACs and biomarkers in

254   saliva and urine (interleukin-6 and 8-hydrox-2′-deoxyguanosine). Zhang et al. (2023)

255   also reported that NACs are major proinflammatory components in organic aerosols,

256   contributing about 24% of the interleukin-8 response of all compounds detected by

257   Fourier transform ion cyclotron resonance mass spectrometry (FT-ICR-MS) in

258   electrospray ionization negative mode (ESI-).

259   The correlation coefficients between DTT$_v$ and 14 trace elements are shown in

260   Figure 4. Generally, the correlations between DTT$_v$ and soluble elements were higher

261 than that between DTT_v and total elements in both the south and north of Beijing,

262 suggesting that the consumption of DTT from elements depend primarily on its

263 soluble fraction instead of their total content. For soluble elements, in the south, the

264 DTT_v showed positive correlations with Mn, Fe, Cr, Co, As and Pb ($r > 0.5$), while in

265 the north, it exhibited strong positive correlations with Mn, Co, Ni, Zn, As, Cd and Pb

266 ($r > 0.7$), indicating the different sources of DTT_v in the south and north of Beijing. It

267 is worth noting that the concentrations of all soluble elements were higher in the south

268 than in the north (Figure S3), while the correlation between DTT_v and most soluble

269 elements was lower in the south than in the north (Figure 4). The high correlations

270 between DTT_v and soluble elements in the north of Beijing suggests that soluble

271 elements also had significant contribution to DTT consumption. The low correlations

272 between DTT_v and soluble elements in the south of Beijing may be due to the

273 nonlinear relationship between DTT consumption and elements concentrations

274 (Charrier and Anastasio, 2012; Wu et al., 2022a).

275 In addition to being associated with individual water-soluble species, the

276 interaction between metal and organic compounds also affects the consumption of

277 DTT (Xiong et al., 2017; Wu et al., 2022b), with both synergistic and antagonistic

278 effects. For example, Wu et al. (2022b) measured the DTT consumption of Fe(III) and

279 Cu(II) interacting with 1,4-naphthoquinone, 9,10-phenanthraquinone, citric acid, and

280 4-nitrocatechol, respectively. Their results showed that Cu(II) had antagonistic effects

281 in interacting with most organics except for citric acid, and Fe(III) had an additive

282 effect on DTT consumption of 1,4-naphthoquinone and citric acid, while it had an

283 antagonistic effect on 1,4-naphthoquinone and 9,10-phenanthraquinone. Due to the

284 complex composition of water-soluble organic aerosols, the knowledge about the

285 effects of organics and metal-organic interactions on DTT activity are still limited,

286 especially the effects of BrC chromophores and their interactions with metals.

287 3.3 Sources of DTT activity

288 The PMF model was applied to quantify the sources of DTT_v in the south and the

289 north of Beijing, which was widely used for the source apportionment of $PM_{2.5}$ OP

290   (Liu et al., 2018; Shen et al., 2022; Cui et al., 2023). The input species include DTT_v,

291   soluble elements, and organic markers (including levoglucosan, mannosan, and

292   galactosan for biomass burning, hopanes for vehicle emissions, picene for coal

293   combustion, and phthalic acid, isophthalic acid and terephthalic acid for secondary

294   formation). The correlation coefficients between DTT_v and organic markers are

295   shown in Figure S4. In the south, levoglucosan, mannosan, galactosan, and hopanes

296   had moderate correlation with DTT_v (r of 0.41 to 0.48); phthalic acid, isophthalic acid

297   and terephthalic acid had low to moderate correlation with DTT_v (r of 0.28 to 0.54);

298   picene had low correlation with DTT_v (r of 0.21). These results suggest that biomass

299   burning and vehicle emissions could have significant contribution to water-soluble

300   $PM_{2.5}$ OP in the south. In the north, hopanes had the highest correlation with DTT_v (r

301   = 0.70), indicating that vehicle emissions could have an important contribution.

302   Levoglucosan, mannosan, galactosan, phthalic acid, isophthalic acid, terephthalic acid,

303   and picene had moderate to high correlations with DTT_v in the north, suggesting that

304   biomass and coal burning, and secondary formation may also have certain

305   contribution to water-soluble $PM_{2.5}$ OP.

306   Six factors were resolved in the south and north of Beijing, including biomass

307   burning, coal burning, traffic-related, dust, oil combustion, and secondary formation,

308   and the profiles of these sources are shown in Figure S5. Factor 1 is characterized by

309   high contribution of levoglucosan, mannosan, and galactosan, mainly from biomass

310   burning (Huang et al., 2014; Chow et al., 2022). The DTT activity of biomass burning

311   organic aerosol was measured by Wong et al. (2019), which was 48 ± 6 pmol min^{-1}

312   μg^{-1} of WSOC. Liu et al. (2018) quantified the sources of DTT_v in coastal cities

313   (Jinzhou, Tianjin, and Yantai) in China with PMF model and multiple linear

314   regression method, and the results showed that biomass burning contributed 27.8% on

315   average in wither. Factor 2 exhibits a large fraction of picene, Zn, Mn, Cd, As, and Pb,

316   which is considered to be coal burning (Huang et al., 2014; Huang et al., 2018). Joo et

317   al. (2018) measured the DTT activity of $PM_{2.5}$ emitted from coal combustion at

318   different temperatures, with the highest values of 26.2 ± 20.5 pmol min^{-1} μg^{-1} and

319   0.10 ± 0.06 nmol min^{-1} m^{-3} occurring at 550 °C. Factor 3 is identified as traffic-related

320   emissions, which is characterized by the higher loading of hopanes, Ba, Sr, Cu and Ni

321   (Huang et al., 2018; Chow et al., 2022). Vreeland et al. (2017) measured the DTT

322   activity of PM$_{2.5}$ emitted by side street and highway vehicles in Atlanta, with values

323   of 0.78 ± 0.60 nmol min^{-1} m^{-3} and 1.08 ± 0.60 nmol min^{-1} m^{-3}, respectively. Ting et al.

324   (2023) reported that the DTT activity of PM$_{2.5}$ from vehicle emissions in Ziqing

325   tunnel in Taiwan, China, was 0.15-0.46 nmol min^{-1} m^{-3}. Factor 4, secondary formation,

326   which is identified by high levels of phthalic acid, isophthalic acid, and terephthalic

327   acid (Al-Naiema and Stone, 2017; Wang et al., 2020a). Verma et al. (2014) reported

328   that secondary formation contributed about 30% to the water-soluble DTT activity of

329   PM$_{2.5}$ in urban Atlanta. It is worth noting that the DTT activity of SOA generated

330   from different precursors is different (Tuet et al., 2017; Tong et al., 2018). For

331   example, the DTT activity of SOA from naphthalene was higher than that from

332   isoprene (Tuet et al., 2017; Tong et al., 2018). Factor 5 is dominated by crustal

333   elements Fe and Ti, mainly from dust (Huang et al., 2018). The DTT activity of

334   atmospheric particulate matter during dust periods were reported in previous studies

335   (Chirizzi et al., 2017; Khoshnamvand et al., 2023) and it has a low contribution in this

336   study. Factor 6 is identified as oil combustion because of the high levels of V and Ni

337   (Moreno et al., 2011; Minguillón et al., 2014; Huang et al., 2018).

338   The source contributions of DTT$_v$ in the south and north of Beijing are shown in

339   Figure 5, exhibiting obvious regional differences. In the south, traffic-related

340   emissions (39.1%) and biomass burning (25.2%) had the most contribution to DTT$_v$,

341   followed by secondary formation (17.2%), coal burning (15%), dust (2%), and oil

342   combustion (1.5%). In the north, traffic-related emissions (51.6%) had the highest

343   contribution to DTT$_v$, followed by coal burning (19.9%), secondary formation (13%),

344   biomass burning (8.4%), oil combustion (4.1%), and dust (3%). The large regional

345   differences in sources of DTT$_v$ of water-soluble PM$_{2.5}$ call for more research on the

346   relationship between sources, chemical composition, formation processes and OP of

347   PM$_{2.5}$.

4 Conclusions

In this study, the water-soluble OP of ambient $PM_{2.5}$ collected in winter in the south and north of Beijing were quantified, together with the concentration and light absorption of WSOC, and concentrations of 7 light-absorbing NACs and 14 trace elements. The average DTT_v value was comparable in the south (3.9 ± 0.9 nmol min^{-1} m^{-3}) and north (3.5 ± 1.2 nmol min^{-1} m^{-3}), while the DTT_m was higher in the north (65.3 ± 27.6 pmol min^{-1} μg^{-1}) than in the south (36.1 ± 14.5 pmol min^{-1} μg^{-1}), indicating that the $PM_{2.5}$ exposure-relevant toxicity was similar in the two sites and that the $PM_{2.5}$ intrinsic toxicity was higher in the north than in the south. The correlation between DTT_v and soluble elements was higher than that between DTT_v and total elements in both the south and north. In the north, the DTT_v was strongly correlated with soluble Mn, Co, Ni, Zn, As, Cd and Pb ($r > 0.7$), and in the south it positively correlated with Mn, Fe, Cr, Co, As and Pb ($r > 0.5$). In addition, in the north the DTT_v was also positively correlated with WSOC, Abs_{365} and NACs (r of 0.56 to 0.79), while in the south it was weakly correlated ($r \leq 0.4$). These results indicate that in the north trace elements and water-soluble organic compounds, especially BrC chromophores, both had significant contributions to DTT consumption, and in the south the consumption of DTT may be mainly from trace elements. Six sources of DTT_v were resolved with the PMF model, including biomass burning, coal burning, traffic-related, dust, oil combustion, and secondary formation. On average, traffic-related emissions (39.1%) and biomass burning (25.2%) were the major contributors of DTT_v in the south, and traffic-related emissions (51.6%) was the predominated source in the north. The differences in DTT_v sources in the south and north of Beijing suggest that the relationship between source emissions and atmospheric processes and $PM_{2.5}$ OP deserve further exploration in order to better understand the regional differences of health impacts of $PM_{2.5}$.

377

Date availability. Raw data used in this study can be obtained from the following open link: https://doi.org/10.5281/zenodo.10791126 (Yuan et al., 2024). It is also available on request by contacting the corresponding author.

381

Supplement. The Supplement related to this article is available online.

383

Author contributions. RJH designed the study. Data analysis was done by WY, CL, LY, HY and RJH. WY, CL, LY, HY and RJH interpreted data, prepared the display items and wrote the manuscript. All authors commented on and discussed the manuscript.

388

Competing interests. The authors declare that they have no conflict of interest.

390

Acknowledgements. We are very grateful to the National Natural Science Foundation of China (NSFC) under Grant No. 41925015, the Strategic Priority Research Program of Chinese Academy of Sciences (XDB40000000), the Key Research Program of Frontier Sciences from the Chinese Academy of Sciences (ZDBS-LY-DQC001), the New Cornerstone Science Foundation through the XPLORER PRIZE, and the Postdoctoral Fellowship Program of CPSF (no. GZC20232628) supported this study.

397

Financial support. This work was supported by the National Natural Science Foundation of China (NSFC) under Grant No. 41925015, the Strategic Priority Research Program of Chinese Academy of Sciences (XDB40000000), the Key Research Program of Frontier Sciences from the Chinese Academy of Sciences (ZDBS-LY-DQC001), the New Cornerstone Science Foundation through the XPLORER PRIZE, and the Postdoctoral Fellowship Program of CPSF (no. GZC20232628).

405

406

407 **References**

408 Ahmad, M., Yu, Q., Chen, J., Cheng, S., Qin, W., and Zhang, Y.: Chemical

409   characteristics, oxidative potential, and sources of $PM_{2.5}$ in wintertime in

410   Lahore and Peshawar, Pakistan, J. Environ. Sci., 102, 148-158,

411   10.1016/j.jes.2020.09.014, 2021.

412 Al-Naiema, I. M. and Stone, E. A.: Evaluation of anthropogenic secondary organic

413   aerosol tracers from aromatic hydrocarbons, Atmos. Chem. Phys., 17, 2053-

414   2065, 10.5194/acp-17-2053-2017, 2017.

415 An, Z., Huang, R. J., Zhang, R., Tie, X., Li, G., Cao, J., Zhou, W., Shi, Z., Han, Y., Gu,

416   Z., and Ji, Y.: Severe haze in northern China: A synergy of anthropogenic

417   emissions and atmospheric processes, Proc. Natl. Acad. Sci. U. S. A., 116,

418   8657-8666, 10.1073/pnas.1900125116, 2019.

419 Bates, J. T., Fang, T., Verma, V., Zeng, L., Weber, R. J., Tolbert, P. E., Abrams, J. Y.,

420   Sarnat, S. E., Klein, M., Mulholland, J. A., and Russell, A. G.: Review of

421   Acellular Assays of Ambient Particulate Matter Oxidative Potential: Methods

422   and Relationships with Composition, Sources, and Health Effects, Environ.

423   Sci. Technol., 53, 4003-4019, 10.1021/acs.est.8b03430, 2019.

424 Burnett, R., Chen, H., Szyszkowicz, M., Fann, N., Hubbell, B., Pope, C. A., 3rd, Apte,

425   J. S., Brauer, M., Cohen, A., Weichenthal, S., Coggins, J., Di, Q., Brunekreef,

426   B., Frostad, J., Lim, S. S., Kan, H., Walker, K. D., Thurston, G. D., Hayes, R.

427   B., Lim, C. C., Turner, M. C., Jerrett, M., Krewski, D., Gapstur, S. M., Diver,

428   W. R., Ostro, B., Goldberg, D., Crouse, D. L., Martin, R. V., Peters, P., Pinault,

429   L., Tjepkema, M., van Donkelaar, A., Villeneuve, P. J., Miller, A. B., Yin, P.,

430   Zhou, M., Wang, L., Janssen, N. A. H., Marra, M., Atkinson, R. W., Tsang, H.,

431   Quoc Thach, T., Cannon, J. B., Allen, R. T., Hart, J. E., Laden, F., Cesaroni, G.,

432   Forastiere, F., Weinmayr, G., Jaensch, A., Nagel, G., Concin, H., and Spadaro,

433   J. V.: Global estimates of mortality associated with long-term exposure to

434   outdoor fine particulate matter, Proc. Natl. Acad. Sci. U. S. A., 115, 9592-9597,

435   10.1073/pnas.1803222115, 2018.

436   Calas, A., Uzu, G., Kelly, F. J., Houdier, S., Martins, J. M. F., Thomas, F., Molton, F.,
437   Charron, A., Dunster, C., Oliete, A., Jacob, V., Besombes, J.-L., Chevrier, F.,
438   and Jaffrezo, J.-L.: Comparison between five acellular oxidative potential
439   measurement assays performed with detailed chemistry on PM$_{10}$ samples from
440   the city of Chamonix (France), Atmos. Chem. Phys., 18, 7863-7875,
441   10.5194/acp-18-7863-2018, 2018.

442   Campbell, S. J., Wolfer, K., Utinger, B., Westwood, J., Zhang, Z. H., Bukowiecki, N.,
443   Steimer, S. S., Vu, T. V., Xu, J., Straw, N., Thomson, S., Elzein, A., Sun, Y.,
444   Liu, D., Li, L., Fu, P., Lewis, A. C., Harrison, R. M., Bloss, W. J., Loh, M.,
445   Miller, M. R., Shi, Z., and Kalberer, M.: Atmospheric conditions and
446   composition that influence PM$_{2.5}$ oxidative potential in Beijing, China, Atmos.
447   Chem. Phys., 21, 5549-5573, 10.5194/acp-21-5549-2021, 2021.

448   Cao, T., Li, M., Zou, C., Fan, X., Song, J., Jia, W., Yu, C., Yu, Z., and Peng, P. a.:
449   Chemical composition, optical properties, and oxidative potential of water-
450   and methanol-soluble organic compounds emitted from the combustion of
451   biomass materials and coal, Atmos. Chem. Phys., 21, 13187-13205,
452   10.5194/acp-21-13187-2021, 2021.

453   Charrier, J. G. and Anastasio, C.: On dithiothreitol (DTT) as a measure of oxidative
454   potential for ambient particles: evidence for the importance of soluble
455   transition metals, Atmos. Chem. Phys., 12, 9321-9333, 10.5194/acp-12-9321-
456   2012, 2012.

457   Chen, K., Xu, J., Famiyeh, L., Sun, Y., Ji, D., Xu, H., Wang, C., Metcalfe, S. E., Betha,
458   R., Behera, S. N., Jia, C., Xiao, H., and He, J.: Chemical constituents, driving
459   factors, and source apportionment of oxidative potential of ambient fine
460   particulate matter in a Port City in East China, J. Hazard. Mater., 440,
461   10.1016/j.jhazmat.2022.129864, 2022.

462   Chen, Q., Wang, M., Wang, Y., Zhang, L., Li, Y., and Han, Y.: Oxidative Potential of
463   Water-Soluble Matter Associated with Chromophoric Substances in PM$_{2.5}$

464 over Xi'an, China, Environ. Sci. Technol., 53, 8574-8584,
465 10.1021/acs.est.9b01976, 2019.

466 Chirizzi, D., Cesari, D., Guascito, M. R., Dinoi, A., Giotta, L., Donateo, A., and
467 Contini, D.: Influence of Saharan dust outbreaks and carbon content on
468 oxidative potential of water-soluble fractions of $PM_{2.5}$ and PM_{10}, Atmos.
469 Environ., 163, 1-8, 10.1016/j.atmosenv.2017.05.021, 2017.

470 Chow, W. S., Huang, X. H. H., Leung, K. F., Huang, L., Wu, X., and Yu, J. Z.:
471 Molecular and elemental marker-based source apportionment of fine
472 particulate matter at six sites in Hong Kong, China, Sci. Total Environ., 813,
473 152652, 10.1016/j.scitotenv.2021.152652, 2022.

474 Chowdhury, P. H., He, Q., Carmieli, R., Li, C., Rudich, Y., and Pardo, M.: Connecting
475 the Oxidative Potential of Secondary Organic Aerosols with Reactive Oxygen
476 Species in Exposed Lung Cells, Environ. Sci. Technol., 53, 13949-13958,
477 10.1021/acs.est.9b04449, 2019.

478 Cui, Y., Zhu, L., Wang, H., Zhao, Z., Ma, S., and Ye, Z.: Characteristics and Oxidative
479 Potential of Ambient $PM_{2.5}$ in the Yangtze River Delta Region: Pollution Level
480 and Source Apportionment, Atmosphere, 14, 10.3390/atmos14030425, 2023.

481 Daellenbach, K. R., Uzu, G., Jiang, J., Cassagnes, L. E., Leni, Z., Vlachou, A.,
482 Stefenelli, G., Canonaco, F., Weber, S., Segers, A., Kuenen, J. J. P., Schaap, M.,
483 Favez, O., Albinet, A., Aksoyoglu, S., Dommen, J., Baltensperger, U., Geiser,
484 M., El Haddad, I., Jaffrezo, J. L., and Prevot, A. S. H.: Sources of particulate-
485 matter air pollution and its oxidative potential in Europe, Nature, 587, 414-419,
486 10.1038/s41586-020-2902-8, 2020.

487 Fan, X., Li, M., Cao, T., Cheng, C., Li, F., Xie, Y., Wei, S., Song, J., and Peng, P. a.:
488 Optical properties and oxidative potential of water- and alkaline-soluble
489 brown carbon in smoke particles emitted from laboratory simulated biomass
490 burning, Atmos. Environ., 194, 48-57, 10.1016/j.atmosenv.2018.09.025, 2018.

491 Fang, T., Verma, V., Bates, J. T., Abrams, J., Klein, M., Strickland, M. J., Sarnat, S. E.,
492 Chang, H. H., Mulholland, J. A., Tolbert, P. E., Russell, A. G., and Weber, R. J.:

Oxidative potential of ambient water-soluble $PM_{2.5}$ in the southeastern United States: contrasts in sources and health associations between ascorbic acid (AA) and dithiothreitol (DTT) assays, Atmos. Chem. Phys., 16, 3865-3879, 10.5194/acp-16-3865-2016, 2016.

Feng, R., Xu, H., Gu, Y., Wang, Z., Han, B., Sun, J., Liu, S., Lu, H., Ho, S. S. H., Shen, Z., and Cao, J.: Variations of Personal Exposure to Particulate Nitrated Phenols from Heating Energy Renovation in China: The First Assessment on Associated Toxicological Impacts with Particle Size Distributions, Environ. Sci. Technol., 56, 3974−3983, 2022.

Gao, D., Fang, T., Verma, V., Zeng, L., and Weber, R. J.: A method for measuring total aerosol oxidative potential (OP) with the dithiothreitol (DTT) assay and comparisons between an urban and roadside site of water-soluble and total OP, Atmos. Meas. Tech., 10, 2821-2835, 10.5194/amt-10-2821-2017, 2017.

Hecobian, A., Zhang, X., Zheng, M., Frank, N., Edgerton, E. S., and Weber, R. J.: Water-Soluble Organic Aerosol material and the light-absorption characteristics of aqueous extracts measured over the Southeastern United States, Atmos. Chem. Phys., 10, 5965-5977, 10.5194/acp-10-5965-2010, 2010.

Ho, K. F., Ho, S. S. H., Huang, R.-J., Liu, S. X., Cao, J.-J., Zhang, T., Chuang, H.-C., Chan, C. S., Hu, D., and Tian, L.: Characteristics of water-soluble organic nitrogen in fine particulate matter in the continental area of China, Atmos. Environ., 106, 252-261, 10.1016/j.atmosenv.2015.02.010, 2015.

Huang, R. J., Cheng, R., Jing, M., Yang, L., Li, Y., Chen, Q., Chen, Y., Yan, J., Lin, C., Wu, Y., Zhang, R., El Haddad, I., Prevot, A. S. H., O'Dowd, C. D., and Cao, J.: Source-Specific Health Risk Analysis on Particulate Trace Elements: Coal Combustion and Traffic Emission As Major Contributors in Wintertime Beijing, Environ. Sci. Technol., 52, 10967-10974, 10.1021/acs.est.8b02091, 2018.

Huang, R. J., Yang, L., Shen, J., Yuan, W., Gong, Y., Guo, J., Cao, W., Duan, J., Ni, H., Zhu, C., Dai, W., Li, Y., Chen, Y., Chen, Q., Wu, Y., Zhang, R., Dusek, U.,

O'Dowd, C., and Hoffmann, T.: Water-Insoluble Organics Dominate Brown Carbon in Wintertime Urban Aerosol of China: Chemical Characteristics and Optical Properties, Environ. Sci. Technol., 54, 7836-7847, 10.1021/acs.est.0c01149, 2020.

Huang, R. J., Zhang, Y., Bozzetti, C., Ho, K. F., Cao, J. J., Han, Y., Daellenbach, K. R., Slowik, J. G., Platt, S. M., Canonaco, F., Zotter, P., Wolf, R., Pieber, S. M., Bruns, E. A., Crippa, M., Ciarelli, G., Piazzalunga, A., Schwikowski, M., Abbaszade, G., Schnelle-Kreis, J., Zimmermann, R., An, Z., Szidat, S., Baltensperger, U., El Haddad, I., and Prevot, A. S.: High secondary aerosol contribution to particulate pollution during haze events in China, Nature, 514, 218-222, 10.1038/nature13774, 2014.

Joo, H. S., Batmunkh, T., Borlaza, L. J. S., Park, M., Lee, K. Y., Lee, J. Y., Chang, Y. W., and Park, K.: Physicochemical properties and oxidative potential of fine particles produced from coal combustion, Aerosol Sci. Technol., 52, 1134-1144, 10.1080/02786826.2018.1501152, 2018.

Khoshnamvand, N., Nodehi, R. N., Hassanvand, M. S., and Naddafi, K.: Comparison between oxidative potentials measured of water-soluble components in ambient air PM_1 and $PM_{2.5}$ of Tehran, Iran, Air Qual. Atmos. Hlth., 16, 1311-1320, 10.1007/s11869-023-01343-y, 2023.

Laskin, A., Laskin, J., and Nizkorodov, S. A.: Chemistry of atmospheric brown carbon, Chem. Rev., 115, 4335-4382, 10.1021/cr5006167, 2015.

Lelieveld, S., Wilson, J., Dovrou, E., Mishra, A., Lakey, P. S. J., Shiraiwa, M., Poschl, U., and Berkemeier, T.: Hydroxyl Radical Production by Air Pollutants in Epithelial Lining Fluid Governed by Interconversion and Scavenging of Reactive Oxygen Species, Environ. Sci. Technol., 55, 14069-14079, 10.1021/acs.est.1c03875, 2021.

Lin, P., Bluvshtein, N., Rudich, Y., Nizkorodov, S. A., Laskin, J., and Laskin, A.: Molecular chemistry of atmospheric brown carbon inferred from a nationwide biomass burning event, Environ. Sci. Technol., 51, 11561–11570, 2017.

551   Liu, W., Xu, Y., Liu, W., Liu, Q., Yu, S., Liu, Y., Wang, X., and Tao, S.: Oxidative

552   potential of ambient PM$_{2.5}$ in the coastal cities of the Bohai Sea, northern

553   China: Seasonal variation and source apportionment, Environ. Pollut., 236,

554   514-528, 10.1016/j.envpol.2018.01.116, 2018.

555   Ma, X., Nie, D., Chen, M., Ge, P., Liu, Z., Ge, X., Li, Z., and Gu, R.: The Relative

556   Contributions of Different Chemical Components to the Oxidative Potential of

557   Ambient Fine Particles in Nanjing Area, Int. J. Environ. Res. Public Health, 18,

558   2789, 10.3390/ijerph18062789, 2021.

559   Minguillón, M. C., Cirach, M., Hoek, G., Brunekreef, B., Tsai, M., de Hoogh, K.,

560   Jedynska, A., Kooter, I. M., Nieuwenhuijsen, M., and Querol, X.: Spatial

561   variability of trace elements and sources for improved exposure assessment in

562   Barcelona, Atmos. Environ., 89, 268-281, 10.1016/j.atmosenv.2014.02.047,

563   2014.

564   Moreno, T., Querol, X., Alastuey, A., Reche, C., Cusack, M., Amato, F., Pandolfi, M.,

565   Pey, J., Richard, A., Prévôt, A. S. H., Furger, M., and Gibbons, W.: Variations

566   in time and space of trace metal aerosol concentrations in urban areas and their

567   surroundings, Atmos. Chem. Phys., 11, 9415-9430, 10.5194/acp-11-9415-2011,

568   2011.

569   Oh, S. H., Park, K., Park, M., Song, M., Jang, K. S., Schauer, J. J., Bae, G. N., and

570   Bae, M. S.: Comparison of the sources and oxidative potential of PM$_{2.5}$ during

571   winter time in large cities in China and South Korea, Sci. Total Environ., 859,

572   160369, 10.1016/j.scitotenv.2022.160369, 2023.

573   Paatero, P.: Least squares formation of robust non negative factor analysis,

574   Chemometr. Intell. Lab., 37, 23-35, 1997.

575   Puthussery, J. V., Dave, J., Shukla, A., Gaddamidi, S., Singh, A., Vats, P., Salana, S.,

576   Ganguly, D., Rastogi, N., Tripathi, S. N., and Verma, V.: Effect of Biomass

577   Burning, Diwali Fireworks, and Polluted Fog Events on the Oxidative

578   Potential of Fine Ambient Particulate Matter in Delhi, India, Environ. Sci.

579   Technol., 56, 14605-14616, 10.1021/acs.est.2c02730, 2022.

580   Shen, J., Taghvaee, S., La, C., Oroumiyeh, F., Liu, J., Jerrett, M., Weichenthal, S., Del
581   Rosario, I., Shafer, M. M., Ritz, B., Zhu, Y., and Paulson, S. E.: Aerosol
582   Oxidative Potential in the Greater Los Angeles Area: Source Apportionment
583   and Associations with Socioeconomic Position, Environ. Sci. Technol., 56,
584   17795-17804, 10.1021/acs.est.2c02788, 2022.

585   Ting, Y. C., Chang, P. K., Hung, P. C., Chou, C. C., Chi, K. H., and Hsiao, T. C.:
586   Characterizing emission factors and oxidative potential of motorcycle
587   emissions in a real-world tunnel environment, Environ. Res., 234, 116601,
588   10.1016/j.envres.2023.116601, 2023.

589   Tong, H., Lakey, P. S. J., Arangio, A. M., Socorro, J., Kampf, C. J., Berkemeier, T.,
590   Brune, W. H., Poschl, U., and Shiraiwa, M.: Reactive oxygen species formed
591   in aqueous mixtures of secondary organic aerosols and mineral dust
592   influencing cloud chemistry and public health in the Anthropocene, Faraday
593   Discuss., 200, 251-270, 10.1039/c7fd00023e, 2017.

594   Tong, H., Lakey, P. S. J., Arangio, A. M., Socorro, J., Shen, F., Lucas, K., Brune, W.
595   H., Poschl, U., and Shiraiwa, M.: Reactive Oxygen Species Formed by
596   Secondary Organic Aerosols in Water and Surrogate Lung Fluid, Environ. Sci.
597   Technol., 52, 11642-11651, 10.1021/acs.est.8b03695, 2018.

598   Tuet, W. Y., Chen, Y., Xu, L., Fok, S., Gao, D., Weber, R. J., and Ng, N. L.: Chemical
599   oxidative potential of secondary organic aerosol (SOA) generated from the
600   photooxidation of biogenic and anthropogenic volatile organic compounds,
601   Atmos. Chem. Phys., 17, 839-853, 10.5194/acp-17-839-2017, 2017.

602   Tuet, W. Y., Liu, F., de Oliveira Alves, N., Fok, S., Artaxo, P., Vasconcellos, P.,
603   Champion, J. A., and Ng, N. L.: Chemical Oxidative Potential and Cellular
604   Oxidative Stress from Open Biomass Burning Aerosol, Environ. Sci. Technol.
605   Lett., 6, 126-132, 10.1021/acs.estlett.9b00060, 2019.

606   Verma, V., Fang, T., Xu, L., Peltier, R. E., Russell, A. G., Ng, N. L., and Weber, R. J.:
607   Organic aerosols associated with the generation of reactive oxygen species
608   (ROS) by water-soluble $PM_{2.5}$, Environ. Sci. Technol., 49, 4646-4656,

609   10.1021/es505577w, 2015.

610   Verma, V., Rico-Martinez, R., Kotra, N., King, L., Liu, J., Snell, T. W., and Weber, R.

611   J.: Contribution of water-soluble and insoluble components and their

612   hydrophobic/hydrophilic subfractions to the reactive oxygen species-

613   generating potential of fine ambient aerosols, Environ. Sci. Technol., 46,

614   11384-11392, 10.1021/es302484r, 2012.

615   Verma, V., Fang, T., Guo, H., King, L., Bates, J. T., Peltier, R. E., Edgerton, E.,

616   Russell, A. G., and Weber, R. J.: Reactive oxygen species associated with

617   water-soluble $PM_{2.5}$ in the southeastern United States: spatiotemporal trends

618   and source apportionment, Atmos. Chem. Phys., 14, 12915-12930,

619   10.5194/acp-14-12915-2014, 2014.

620   Vreeland, H., Weber, R., Bergin, M., Greenwald, R., Golan, R., Russell, A. G., Verma,

621   V., and Sarnat, J. A.: Oxidative potential of $PM_{2.5}$ during Atlanta rush hour:

622   Measurements of in-vehicle dithiothreitol (DTT) activity, Atmos. Environ.,

623   165, 169-178, 10.1016/j.atmosenv.2017.06.044, 2017.

624   Wang, J., Lin, X., Lu, L., Wu, Y., Zhang, H., Lv, Q., Liu, W., Zhang, Y., and Zhuang,

625   S.: Temporal variation of oxidative potential of water soluble components of

626   ambient $PM_{2.5}$ measured by dithiothreitol (DTT) assay, Sci. Total Environ.,

627   649, 969-978, 10.1016/j.scitotenv.2018.08.375, 2019.

628   Wang, T., Huang, R. J., Li, Y., Chen, Q., Chen, Y., Yang, L., Guo, J., Ni, H., Hoffmann,

629   T., Wang, X., and Mai, B.: One-year characterization of organic aerosol

630   markers in urban Beijing: Seasonal variation and spatiotemporal comparison,

631   Sci. Total Environ., 743, 140689, 10.1016/j.scitotenv.2020.140689, 2020a.

632   Wang, Y., Wang, M., Li, S., Sun, H., Mu, Z., Zhang, L., Li, Y., and Chen, Q.: Study on

633   the oxidation potential of the water-soluble components of ambient $PM_{2.5}$ over

634   Xi'an, China: Pollution levels, source apportionment and transport pathways,

635   Environ. Int., 136, 105515, 10.1016/j.envint.2020.105515, 2020b.

636   Wong, J. P. S., Tsagkaraki, M., Tsiodra, I., Mihalopoulos, N., Violaki, K., Kanakidou,

637   M., Sciare, J., Nenes, A., and Weber, R. J.: Effects of Atmospheric Processing

hidden

638   on the Oxidative Potential of Biomass Burning Organic Aerosols, Environ. Sci.
639   Technol., 53, 6747-6756, 10.1021/acs.est.9b01034, 2019.

640 Wu, N., Lu, B., Chen, Q., Chen, J., and Li, X.: Connecting the Oxidative Potential of
641   Fractionated Particulate Matter With Chromophoric Substances, J. Geophys.
642   Res-Atmos., 127, 10.1029/2021jd035503, 2022a.

643 Wu, N., Lyu, Y., Lu, B., Cai, D., Meng, X., and Li, X.: Oxidative potential induced by
644   metal-organic interaction from PM$_{2.5}$ in simulated biological fluids, Sci. Total
645   Environ., 848, 157768, 10.1016/j.scitotenv.2022.157768, 2022b.

646 Xing, C., Wang, Y., Yang, X., Zeng, Y., Zhai, J., Cai, B., Zhang, A., Fu, T. M., Zhu, L.,
647   Li, Y., Wang, X., and Zhang, Y.: Seasonal variation of driving factors of
648   ambient PM$_{2.5}$ oxidative potential in Shenzhen, China, Sci. Total Environ., 862,
649   160771, 10.1016/j.scitotenv.2022.160771, 2023.

650 Xiong, Q., Yu, H., Wang, R., Wei, J., and Verma, V.: Rethinking Dithiothreitol-Based
651   Particulate Matter Oxidative Potential: Measuring Dithiothreitol Consumption
652   versus Reactive Oxygen Species Generation, Environ. Sci. Technol., 51, 6507-
653   6514, 10.1021/acs.est.7b01272, 2017.

654 Yu, H., Wei, J., Cheng, Y., Subedi, K., and Verma, V.: Synergistic and Antagonistic
655   Interactions among the Particulate Matter Components in Generating Reactive
656   Oxygen Species Based on the Dithiothreitol Assay, Environ. Sci. Technol., 52,
657   2261–2270, 2018.

658 Yu, Q., Chen, J., Qin, W., Ahmad, M., Zhang, Y., Sun, Y., Xin, K., and Ai, J.:
659   Oxidative potential associated with water-soluble components of PM$_{2.5}$ in
660   Beijing: The important role of anthropogenic organic aerosols, J. Hazard.
661   Mater., 433, 128839, 10.1016/j.jhazmat.2022.128839, 2022a.

662 Yu, S., Liu, W., Xu, Y., Yi, K., Zhou, M., Tao, S., and Liu, W.: Characteristics and
663   oxidative potential of atmospheric PM$_{2.5}$ in Beijing: Source apportionment and
664   seasonal variation, Sci. Total Environ., 650, 277-287,
665   10.1016/j.scitotenv.2018.09.021, 2019.

666 Yu, Y., Sun, Q., Li, T., Ren, X., Lin, L., Sun, M., Duan, J., and Sun, Z.: Adverse

667   outcome pathway of fine particulate matter leading to increased cardiovascular

668   morbidity and mortality: An integrated perspective from toxicology and

669   epidemiology, J. Hazard. Mater., 430, 128368, 10.1016/j.jhazmat.2022.128368,

670   2022b.

671   Yu, Y., Cheng, P., Li, Y., Gu, J., Gong, Y., Han, B., Yang, W., Sun, J., Wu, C., Song,

672   W., and Li, M.: The association of chemical composition particularly the

673   heavy metals with the oxidative potential of ambient $PM_{2.5}$ in a megacity

674   (Guangzhou) of southern China, Environ. Res., 213, 113489,

675   10.1016/j.envres.2022.113489, 2022c.

676   Yuan, W., Huang, R.-J., Luo, C., Yang, L., Cao, W., Guo, J., and Yang, H.:

677   Measurement report: Oxidation potential of water-soluble aerosol components

678   in the southern and northern of Beijing, Zenodo [data set],

679   https://doi.org/10.5281/zenodo.10791126, 2024.

680   Yuan, W., Huang, R.-J., Yang, L., Guo, J., Chen, Z., Duan, J., Wang, T., Ni, H., Han,

681   Y., Li, Y., Chen, Q., Chen, Y., Hoffmann, T., and O'Dowd, C.: Characterization

682   of the light-absorbing properties, chromophore composition and sources of

683   brown carbon aerosol in Xi'an, northwestern China, Atmos. Chem. Phys., 20,

684   5129-5144, 10.5194/acp-20-5129-2020, 2020.

685   Zhang, Q., Ma, H., Li, J., Jiang, H., Chen, W., Wan, C., Jiang, B., Dong, G., Zeng, X.,

686   Chen, D., Lu, S., You, J., Yu, Z., Wang, X., and Zhang, G.: Nitroaromatic

687   Compounds from Secondary Nitrate Formation and Biomass Burning Are

688   Major Proinflammatory Components in Organic Aerosols in Guangzhou: A

689   Bioassay Combining High-Resolution Mass Spectrometry Analysis, Environ.

690   Sci. Technol., 57, 21570-21580, https://doi.org/10.1021/acs.est.3c04983, 2023.

691   Zheng, Y., Davis, S. J., Persad, G. G., and Caldeira, K.: Climate effects of aerosols

692   reduce economic inequality, Nat. Clim. Chang., 10, 220-224, 2020.

693

694

695

696
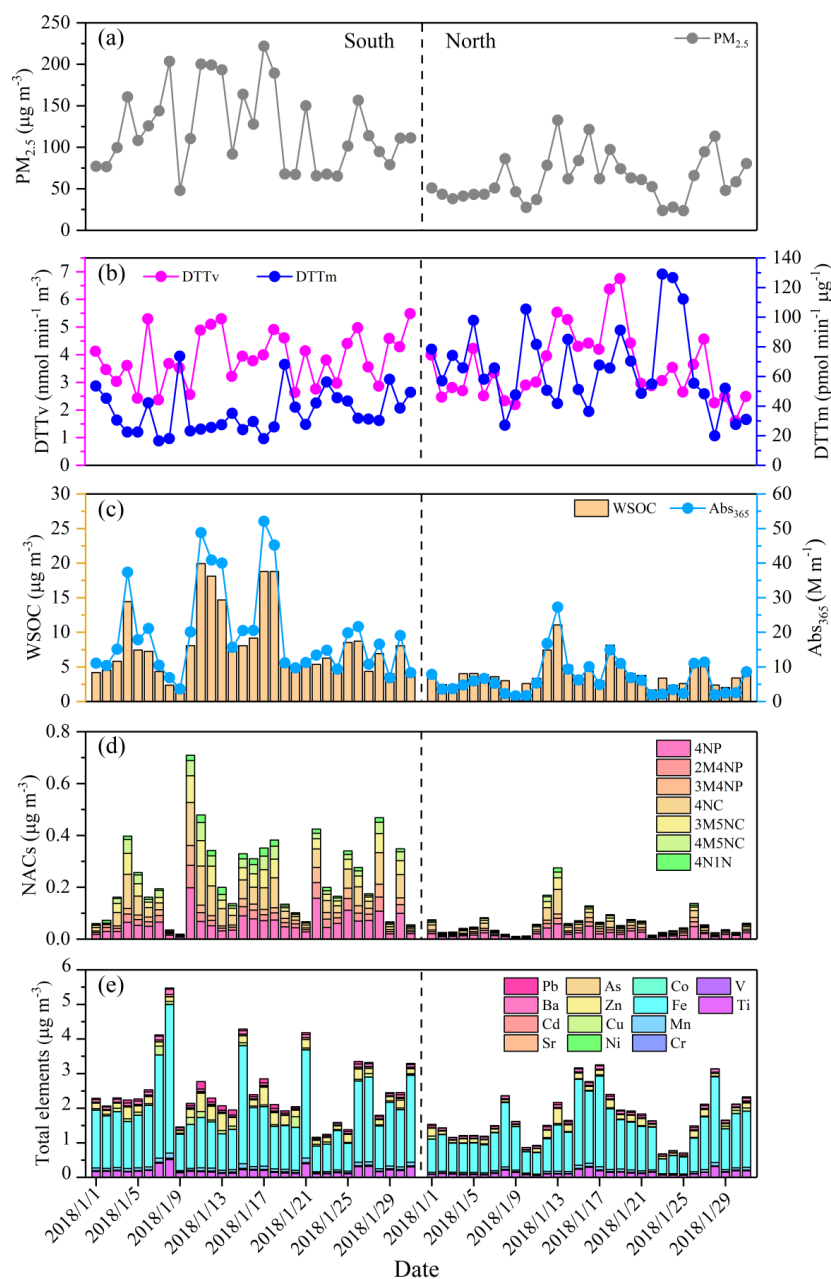
Figure 1. Time series of (a) PM$_{2.5}$ concentration, (b) DTT$_v$ and DTT$_m$, (c) concentration and light absorption at wavelength 365 nm (Abs$_{365}$) of WSOC, concentrations of of (d) NACs and (e) elements.

700

701
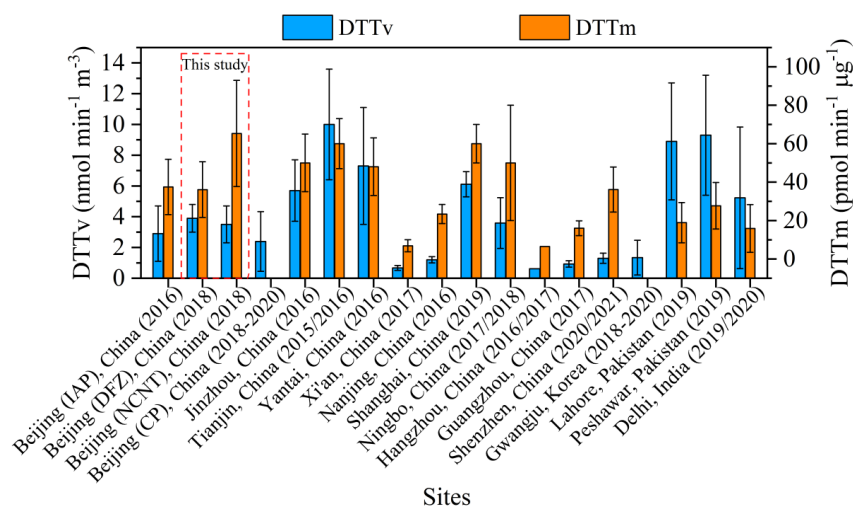
Figure 2. Comparison of DTT_v and DTT_m values measured in this study with those measured in other areas of Asia during similar period.

704

705
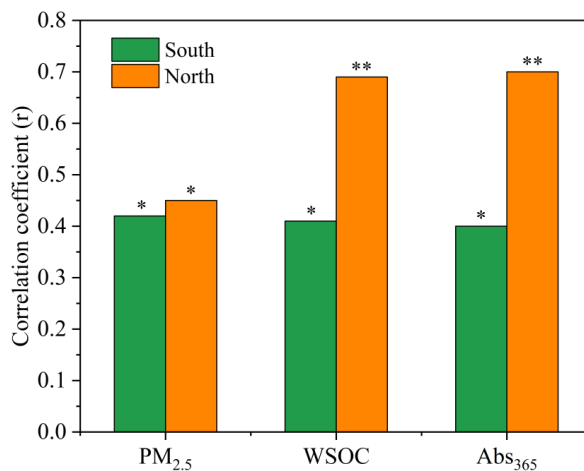
Figure 3. Correlation coefficients between DTT_v and $PM_{2.5}$, WSOC, and Abs_{365} in the south and north of Beijing.

708

709
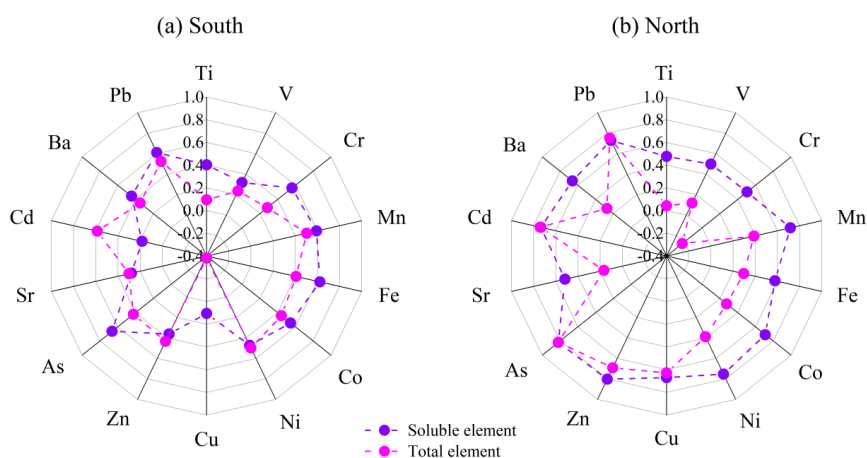
Figure 4. Correlation coefficients between DTT_v and elements in the (a) south and (b)

711 north of Beijing.

712

713
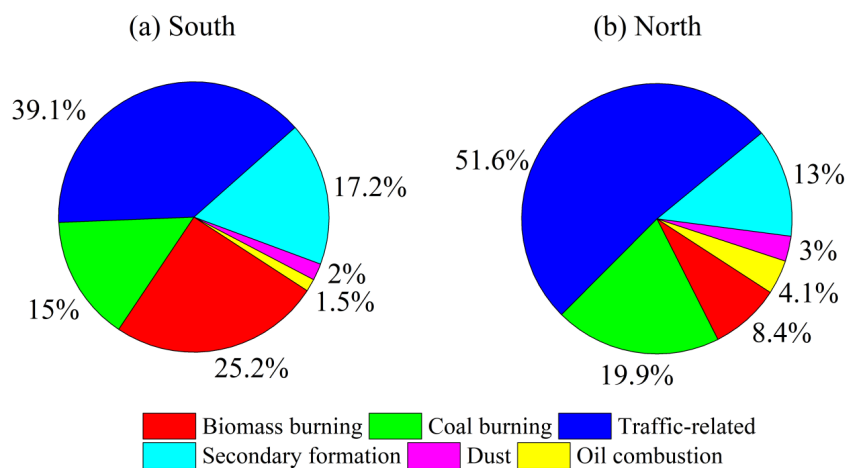
Figure 5. Contributions of resolved sources to DTT_v in the (a) south and (b) north of

715 Beijing.